JOURNAL OF GUIDANCE, CONTROL, AND DYNAMICS
Vol. 18, No. 1, January–February 1995

# Dynamics and Control of a Tethered Flight Vehicle

T. S. No* and J. E. Cochran Jr.†
*Auburn University, Auburn, Alabama 36849-5338*

**Certain types of the problems of dynamics and control of maneuverable tethered flight vehicles are dealt with in this paper. The numerically linearized equations of motion are used in a stability analysis and to design control laws that may be used in station keeping and maneuvering of the vehicle. For motion in which deviations from the equilibrium states are small in magnitude and the maneuver of the vehicle is confined to a neighboring region, the use of a linear quadratic regulator (LQR) for the station keeping and a linear terminal controller for the maneuver is investigated. For the model and conditions used, it is shown that aerodynamic control may be used successfully for station keeping and maneuvering, and the aerodynamic control yields results comparable to those obtained by using reaction control.**

## Introduction

THE dynamics and control of tethered satellite systems (TSSs)[1] have inspired many researchers and matured to the point where one enjoys the ampleness of the pertinent literature. Typical operation of a TSS involves the deployment and retrieval of the subsatellite and station keeping. Because of the inherent instability of the retrieval process, efforts have been focused on the dynamic analysis and synthesis of control laws for TSSs during the deployment and retrieval phases.[2,3]

After the subsatellite is fully deployed, its exact final position is not of concern in most cases. However, if the subsatellite is lowered into the region where the effect of the atmosphere is significant, the uncontrolled motion of the fully deployed TSS configuration could be unstable due to the combined effects of the tether elasticity and the atmospheric density gradient.[4,5]

It has been shown that stabilization can be achieved by modulating the tension in the cable or using the thrusters.[6,7] Also, one may postulate the situation where the position of a deployed subsatellite needs to be corrected and the capability to maneuver the subsatellite is needed. This will be especially important if the main satellite is on an elliptic orbit with nonzero inclination and rotation of the atmosphere is considered. These examples illustrate the station keeping and maneuvering of the subsatellite of a TSS.[1]

Often, subsatellites of TSSs have been modeled as point masses with simplified aerodynamic characteristics, usually drag only. Furthermore, not much attention has been paid to their attitude motion. When the subsatellite is modeled as a rigid body, No and Cochran[8] showed that the motion of the tether and the subsatellite's attitude motion are coupled even if there is no tether attachment point offset from the center of mass of the subsatellite. In the presence of atmospheric effects, not only the tether swinging motion, but also the attitude motion of the subsatellite may become unstable in certain cases. Therefore, it is necessary to consider the motion of the tether and the subsatellite together in the design of control systems.

In view of the above, this paper addresses two problems. First, the dynamics of the motion of a rather general tethered flight vehicle is investigated. The resulting rather complicated equations of motion are numerically linearized for stability analysis and control synthesis. Second, control strategies for station keeping and maneuvering of the tethered flight vehicle are developed by using well-established linear optimal control theory.

Received Dec. 9, 1991; revision received July 20, 1993; accepted for publication March 8, 1994. 

*Graduate Research Assistant, Department of Aerospace Engineering; currently, Senior Research Engineer, Korea Aerospace Research Institute. Student Member AIAA.

†Professor and Head, Department of Aerospace Engineering. Associate Fellow AIAA.

For the purposes of this paper, the subsatellite, modeled as a rigid body located in the region of the sensible atmosphere, is assumed to have physical and aerodynamic characteristics similar to a hypervelocity flight vehicle.[9] Furthermore, the vehicle is assumed to be equipped with conventional control surfaces, e.g., ailerons, elevator, and rudder, so that the aerodynamic forces on the vehicle may be used in controlling the tether motion as well as the vehicle's attitude motion. Such a control system may have restricted capabilities because of the limited magnitude of the aerodynamic forces. However, the use of aerodynamic control may provide some advantages over reaction-type controllers.

## Dynamic Analysis

### Equations of Motion

Shown in Fig. 1 is a sketch of the physical model used in this paper. The motion of the main satellite is assumed to be prescribed and be undisturbed by the motion of the tether and the end body. The mass points $m_j$, $j = 2, 3, \ldots, n$, are used to model the massive tether, whereas $m_1$ is the mass of the rigid body used to model the subsatellite. Each tether segment between point masses is assumed to be massless but extensible.

Referring to Fig. 2, the in-plane and out-of-plane rotations of the $j$th tether segment are specified by the angles $\theta_j$ and $\phi_j$, respectively. We denote by $\sigma_j$ the length of the unstretched tether segment and by $\epsilon_j$ the increase in the tether segment's length due to extension. Using vector notation, we may write the relative position, velocity, and acceleration of the point mass $m_j$ with respect to $m_{j+1}$ as

$$\boldsymbol{r}_j = \boldsymbol{\epsilon}_j + \boldsymbol{\sigma}_j \tag{1}$$

$$\dot{\boldsymbol{r}}_j = \frac{\delta \boldsymbol{\epsilon}_j}{\delta t} + (\boldsymbol{\omega}_j + \boldsymbol{\Omega}_j) \times \boldsymbol{r}_j \tag{2}$$

and

$$\ddot{\boldsymbol{r}}_j = \frac{\delta^2 \boldsymbol{\epsilon}_j}{\delta t^2} + 2(\boldsymbol{\omega}_j + \boldsymbol{\Omega}_p) \times \frac{\delta \boldsymbol{\epsilon}_j}{\delta t} + (\boldsymbol{\omega}_j + \boldsymbol{\Omega}_p) \times [(\boldsymbol{\omega}_j + \boldsymbol{\Omega}_p) \times \boldsymbol{r}_j] + (\dot{\boldsymbol{\omega}}_j + \dot{\boldsymbol{\Omega}}_p) \times \boldsymbol{r}_j \tag{3}$$

respectively, where $\boldsymbol{\Omega}_p$ is the angular velocity of the local vertical coordinate system with respect to the nonrotating coordinate system $EXYZ$ and $\boldsymbol{\omega}_j$ is the angular velocity vector of the $j$th tether-fixed coordinate system $m_{j+1}x_jy_jz_j$ relative to the local vertical system $Px_py_pz_p$.

Now, let us introduce new variables $\boldsymbol{v}_j$, $j = 1, 2, \ldots, n$, by the equation

$$\boldsymbol{v}_j = \dot{\boldsymbol{\epsilon}}_j + \boldsymbol{\omega}_j \times \boldsymbol{r}_j \tag{4}$$

Clearly, $\boldsymbol{v}_j$ is the velocity of $m_j$ as seen in the local vertical frame. The kinematic relationships between tether-fixed components of $v_j$,

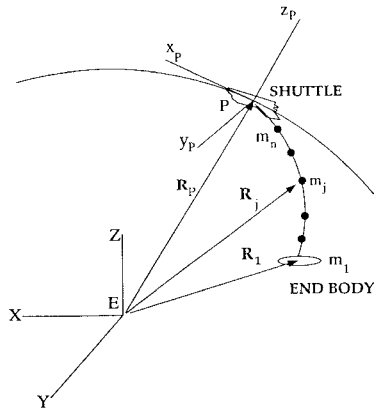


**Fig. 1 TSS model.**

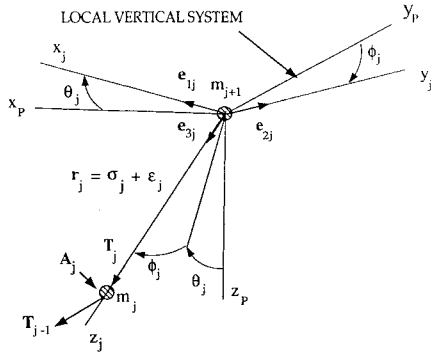


**Fig. 2 Tether notation.**

the $v_{kj}$, $k = 1, 2, 3$, and the angles $\theta_j$ and $\phi_j$ are

$$\dot{\phi}_j = -v_{2j}/(\sigma_j + \epsilon_j), \qquad \dot{\theta}_j = v_{1j}/[(\sigma_j + \epsilon_j)\cos\theta_j] \qquad \dot{\epsilon}_j = v_{3j} \tag{5}$$

To obtain the equations for the tether motion, we follow the procedure given in Ref. 8. Then, we formally write the equations of motion as

$$\boldsymbol{e}_{pi} \cdot \sum_{j=1}^{i} m_j \left( \sum_{k=j}^{n} \dot{\boldsymbol{v}}_k \right) = \boldsymbol{e}_{pi} \cdot T_i - \boldsymbol{e}_{pi} \cdot \sum_{j=1}^{i} m_j \boldsymbol{u}_j + \boldsymbol{e}_{pi} \cdot \sum_{j=1}^{i} (\boldsymbol{A}_j + m_j \boldsymbol{g}_j) - \boldsymbol{e}_{pi} \cdot \left( \sum_{j=1}^{i} m_j \right) \boldsymbol{a}_p + \boldsymbol{e}_{pi} \cdot \boldsymbol{F}_c$$

$$i = 1, 2, \ldots, n, \qquad p = 1, 2, 3 \tag{6}$$

where the following notation is used:

$\boldsymbol{T}_i$ = tension force acting in $i$ tether
$\boldsymbol{u}_j = \sum_{k=j}^{n} [(\omega_k + \Omega_p) \times \boldsymbol{v}_k + \Omega_p \times (\Omega_p \times \boldsymbol{r}_k) + \dot{\Omega}_p \times \boldsymbol{r}_k]$
$\boldsymbol{A}_j$ = aerodynamic force acting on $m_j$
$m_j \boldsymbol{g}_j$ = gravitational force acting on $m_j$
$\boldsymbol{a}_p$ = acceleration vector of orbiting main satellite
$\boldsymbol{F}_c$ = control force acting on $m_1$, the tethered vehicle
$\boldsymbol{e}_{pi}$ = unit vectors in $i$th tethered-fixed coordinates system, $p = 1, 2, 3$.

Using the Euler angles $\Psi$, $\Theta$, and $\Phi$ in a 3-2-1 sequence to specify the attitude of the subsatellite with respect to the inertial system, we obtain the necessary equations for the rotational motion of the vehicle as

$$\begin{bmatrix} \dot{\Phi} \\ \dot{\Theta} \\ \dot{\Psi} \end{bmatrix} = \begin{bmatrix} 1 & \tan\Theta \sin\Phi & \tan\Theta \cos\Phi \\ 0 & \cos\Phi & -\sin\Phi \\ 0 & \sin\Phi/\cos\Theta & \cos\Phi/\cos\Theta \end{bmatrix} \begin{bmatrix} p \\ q \\ r \end{bmatrix} \tag{7}$$

and

$$\boldsymbol{I} \cdot (\dot{\omega} + \dot{\Omega}_p) = -(\omega + \Omega_p) \times \boldsymbol{I} \cdot (\omega + \Omega_p) + \boldsymbol{M}_A + \boldsymbol{M}_g + \boldsymbol{M}_c \tag{8}$$

where $\omega = (p \quad q \quad r)^T$ and $\boldsymbol{I}$ are the angular velocity and the centroidal inertia dyadic, respectively, of the tethered vehicle. Here $\boldsymbol{M}_A, \boldsymbol{M}_g$, and $\boldsymbol{M}_c$ represent, respectively, aerodynamic, gravity-gradient, and control moments acting on the vehicle.

Equations (5–8) are the equations needed to describe the motion of maneuverable tethered flight vehicles during the station keeping and maneuvers. The resulting equations of motion are highly nonlinear and coupled but may be written in matrix form as

$$\dot{\boldsymbol{X}} = \boldsymbol{F}(\boldsymbol{X}, \boldsymbol{u}) \tag{9}$$

where $\boldsymbol{X}$ is the state vector, explicitly given by

$$\boldsymbol{X} = (\phi_1 \ \theta_1 \ \epsilon_1 \ \phi_2 \ \theta_2 \ \epsilon_2 \cdots \phi_n \ \theta_n \ \epsilon_n \ \Phi \ \Theta \ \Psi \ v_{11} \ v_{21} \ v_{31} \ v_{12} \ v_{22} \ v_{32} \cdots p \ q \ r)^T$$

and $\boldsymbol{u}$ is the control vector that will be described in the next section.

**Forces and Moments Acting on Tethered Vehicle**

Because the tethered subsatellite is modeled as a rigid body, the forces and moments acting on it will differ from those on a point-mass model. Here, we will follow Drummond[9] and assume that the aerodynamic force and moment on the vehicle

$$\boldsymbol{A}_1 = \tfrac{1}{2}\rho V^2 S C_x \boldsymbol{i}_w + \tfrac{1}{2}\rho V^2 S C_y \boldsymbol{j}_w + \tfrac{1}{2}\rho V^2 S C_z \boldsymbol{k}_w \tag{10}$$

$$\boldsymbol{M}_A = \tfrac{1}{2}\rho V^2 S C_l \left(\tfrac{1}{2}b\right)\boldsymbol{i}_b + \tfrac{1}{2}\rho V^2 S C_m \left(\tfrac{1}{2}c\right)\boldsymbol{j}_b + \tfrac{1}{2}\rho V^2 S C_n \left(\tfrac{1}{2}b\right)\boldsymbol{k}_b \tag{11}$$

are, respectively, in the wind-fixed frame and in the vehicle's body-fixed frame. The unit vectors $\boldsymbol{i}_w, \boldsymbol{j}_w$, and $\boldsymbol{k}_w$ are used to denote the unit vectors in the wind-fixed coordinate system, which has its $x_w$ axis aligned with the negative of the relative wind seen by the vehicle. Also, $\boldsymbol{i}_b, \boldsymbol{j}_b$, and $\boldsymbol{k}_b$ are unit vectors attached to the body-fixed coordinate system. In Eqs. (10) and (11), the aerodynamic force and moment coefficients are functions of angle of attack $\alpha$, sideslip angle $\beta$, and angular velocity components $p$ (roll rate), $q$ (pitch rate), and $r$ (yaw rate), and are defined as follows:

$$C_x = -C_D, \qquad C_y = C_{y_\beta}\beta + C_{y_p}p + C_{y_r}r, \qquad C_z = C_{z_\alpha}\alpha + C_{z_q}q$$

$$C_l = C_{l_\beta}\beta + C_{l_p}p + C_{l_r}r, \qquad C_m = C_{m_\alpha}\alpha + C_{m_q}q, \qquad C_n = C_{n_\beta}\beta + C_{n_p}p + C_{n_r}r$$

where Drummond's notation[9] for the stability derivatives is used. Also, $\rho$ is the atmospheric density, which is a function of the altitude of the tethered vehicle; $V$ is the relative wind speed; and $S$, $c$, and $b$ are, respectively, the characteristic area and lengths for the aerodynamics. The expression for the gravity-gradient torque $\boldsymbol{M}_g$ may be found in Ref. 8.

Two controllers are considered in this paper. One is based on the use of aerodynamic control and the other on reaction-type control. Assuming that the vehicle is equipped with an elevator ($\delta_e$), a rudder ($\delta_r$), and ailerons ($\delta_a$), we may write the aerodynamic force and moment due to control as

$$\boldsymbol{F}_c = \tfrac{1}{2}\rho V^2 S C_{y_{\delta_r}} \delta_r \boldsymbol{j}_w + \tfrac{1}{2}\rho V^2 S C_{z_{\delta_e}} \delta_e \boldsymbol{k}_w \tag{12}$$

$$\boldsymbol{M}_c = \tfrac{1}{2}\rho V^2 S b C_{l_{\delta_a}} \delta_a \boldsymbol{i}_b + \tfrac{1}{2}\rho V^2 S c C_{m_{\delta_e}} \delta_e \boldsymbol{j}_b + \tfrac{1}{2}\rho V^2 S b C_{n_{\delta_r}} \delta_r \boldsymbol{k}_b \tag{13}$$

respectively. For the reaction-type controller, we set $\boldsymbol{F}_c = T_x\boldsymbol{i}_b + T_y\boldsymbol{j}_b + T_z\boldsymbol{k}_b$ and $\boldsymbol{M}_c = T_l\boldsymbol{i}_b + T_m\boldsymbol{j}_b + T_n\boldsymbol{k}_b$, where $T_x$, $T_y$, and $T_z$ are thrusting forces along $x$, $y$, and $z$ directions, respectively, and $T_l$, $T_m$, and $T_n$ are control torque components about the $x$, $y$, and $z$ axes, respectively.

**Linear Equations of Motion**

An attempt to analyze the motion of the system by using the equations of motion [Eqs. (5–8)] obtained in the previous section may be costly and impractical unless these equations are very much simplified. No and Cochran[8] suggested that a numerical approach based on standard mathematics may be used to perform stability analyses by obtaining equations for motion about equilibrium states of the complicated TSS model. In this paper, we extend this technique and apply it to study the problem of TSS station keeping and maneuvers of the tethered vehicle (subsatellite).

Following the procedure described in Ref. 8, the equations that govern motion about an equilibrium state $\boldsymbol{X}_e$ may be written in the form

$$\dot{\boldsymbol{x}} = \boldsymbol{A}\boldsymbol{x} + \boldsymbol{B}\boldsymbol{u} \tag{14}$$

where $\boldsymbol{x} = \boldsymbol{X} - \boldsymbol{X}_e$ is the deviation of the states from their equilibrium values and $\boldsymbol{u}$ is the control vector. Aerodynamic trim at zero control deflection ($\delta_e = \delta_r = \delta_a = 0$) is assumed. For the aerodynamic control $\boldsymbol{u} = (\delta_e\ \delta_r\ \delta_a)^T$, and for the reaction control $\boldsymbol{u} = (T_x\ T_y\ T_z\ T_l\ T_m\ T_n)^T$.

To illustrate the effectiveness of the numerical linearization, Eqs. (9) and (14) were integrated to get the response of the uncontrolled motion following initial perturbations. Our first example is a simple case for which $n = 1$ in Eq. (6). In other words, the tether is modeled as a straight and massless but extensible cable segment and the aerodynamic force on the tether is neglected. The orbit of the main body is assumed to be equatorial and circular with a radius of 6578 km. The mass properties and aerodynamic characteristics of the tethered vehicle are given in Table 1. The system matrix $\boldsymbol{A}$ and its eigenvalues are given in Table 2.

Time histories of the representative variables are presented in Figs. 3–5. For this example, the equilibrium states were perturbed by using the initial impulses of $\theta_1 = \phi_1 = 0.0001$ rad/s and $q = r = 0.01$ rad/s. In general, the results from the linear and nonlinear simulations are in good agreement. This implies that the nonlinear equations of motion have been numerically linearized with reasonable accuracy. From Figs. 3 and 4, we see that the in-plane motion looks slightly unstable, whereas the out-of-plane motion is apparently stable, but not asymptotically stable. These conclusions are supported by the fact that the real parts of some eigenvalues of $\boldsymbol{A}$ are positive. By looking at the elements of matrix $\boldsymbol{A}$, we note that the longitudinal motion (in-plane, longitudinal vibration and pitch motion) and the lateral motion (out-of-plane, yaw and roll motion) are uncoupled in the linear sense. During the time of simulation shown in Fig. 5, the pitching motion of the vehicle looks stable, but it may become unstable because of the unstable in-plane motion.

**Table 1 Physical and aerodynamic characteristics of TSS system**

Physical properties of tethered vehicle:

$m_1 = 400$ kg, $I_{xx} = 17.4$ kg-m$^2$, $I_{yy} = 87.0$ kg-m$^2$, $I_{zz} = 97.5$ kg-m$^2$
Reference area $S = 1.3$ m$^2$
Reference lengths: $c = 2.29$ m, $b = 1.13$ m
Unstretched length of tether = 100 km
Tether stiffness EA = $10^4$ N

Aerodynamic characteristics:

| | | | |
|---|---|---|---|
| $C_D = 2.2$ | $C_{y_\beta} = -0.5$ | $C_{y_p} = -0.1$ | $C_{y_r} = -0.1$ |
| $C_{z_\alpha} = -1.0$ | $C_{z_q} = -0.1$ | $C_{l_\beta} = -0.1$ | $C_{l_p} = -0.2$ |
| $C_{l_r} = -0.2$ | $C_{m_\alpha} = -0.5$ | $C_{m_q} = -0.1$ | $C_{n_\beta} = 0.17$ |
| $C_{n_p} = -0.2$ | $C_{n_r} = -1.4$ | | |

Aerodynamic control effectiveness:

| | | |
|---|---|---|
| $C_{y_{\delta_r}} = 1.0$ | $C_{z_{\delta_e}} = -1.0$ | |
| $C_{l_{\delta_a}} = 1.0$ | $C_{m_{\delta_e}} = -1.0$ | $C_{n_{\delta_r}} = 1.0$ |

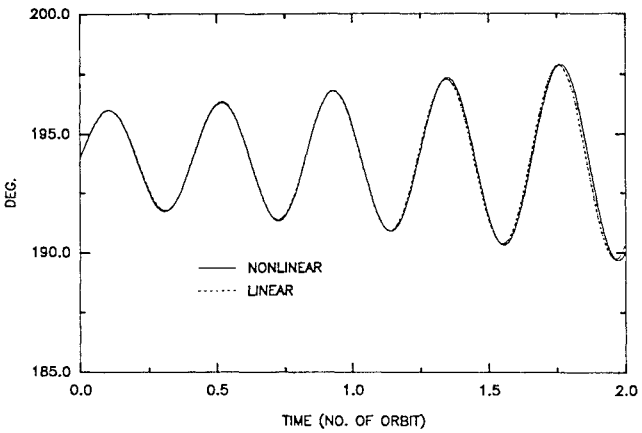


**Fig. 3 Time history of in-plane motion.**

**Table 2 System matrix and eigenvalues**

Matrix $\boldsymbol{A}$

| | | | | | | | | | | | |
|---|---|---|---|---|---|---|---|---|---|---|---|
| 0 | 0 | 0 | 0 | 0 | 0 | 0 | −0.01 | 0 | 0 | 0 | 0 |
| 0 | 0 | 0 | 0 | 0 | 0 | 0.01 | 0 | 0 | 0 | 0 | 0 |
| 0 | 0 | 0 | 0 | 0 | 0 | 0 | 0 | 1 | 0 | 0 | 0 |
| 0 | 0 | 0 | 0 | 0 | 0 | 0 | 0 | 0 | 1 | 0 | −0.004 |
| 0 | 0 | 0 | 0 | 0 | 0 | 0 | 0 | 0 | 0 | 1 | 0 |
| 0 | 0 | 0 | 0 | 0 | 0 | 0 | 0 | 0 | 0 | 0 | 1 |
| 0 | −0.001 | 0 | 0 | 0 | 0 | 0 | 0 | −0.002 | 0 | 0 | 0 |
| 0.001 | 0 | 0 | 0 | 0 | 0 | 0 | 0 | 0 | 0 | 0 | 0 |
| 0 | 0 | 0 | 0 | 0 | 0 | 0.002 | 0 | 0 | 0 | 0 | 0 |
| 0 | 0 | 0 | 0 | 0 | 0.063 | 0 | −0.008 | 0 | −0.125 | 0 | −0.126 |
| 0 | 0 | 0 | 0 | −0.01 | 0 | 0 | 0 | 0.001 | 0 | −0.025 | 0 |
| 0 | 0 | 0 | 0 | 0 | -0.019 | 0 | 0.002 | 0 | −0.23 | 0 | −0.157 |

Eigenvalues

$-0.1994$
$-4.1369 \times 10^{-2} \pm 0.1325i$
$-6.9354 \times 10^{-6} \pm 2.3943 \times 10^{-3}i$
$1.6366 \times 10^{-5}$
$-1.2707 \times 10^{-2} \pm 9.9989 \times 10^{-2i}$
$-9.4963 \times 10^{-5} \pm 1.5729 \times 10^{-2i}$
$7.4226 \times 10^{-5} \pm 2.8655 \times 10^{-3i}$

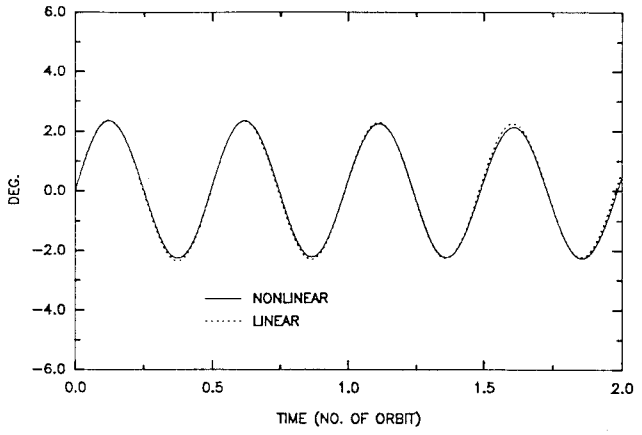


**Fig. 4 Time history of out-of-plane motion.**

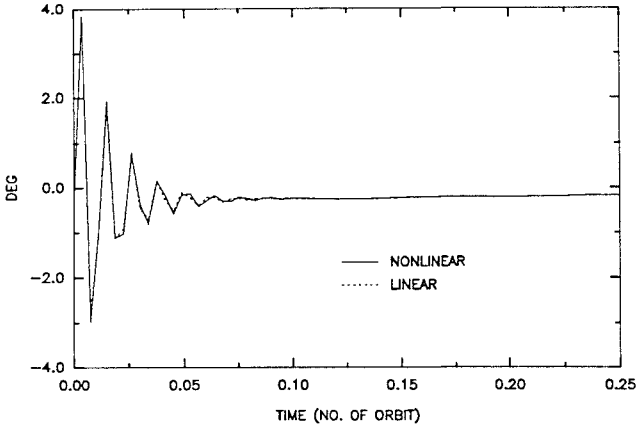


**Fig. 5 Time history of vehicle's pitch motion.**

## Control Synthesis

Because of the low atmospheric density, perturbations due to the atmospheric forces will be small. Likewise, the basic restoring and control forces will be small. However, the deviation from the equilibrium state and maneuvers to a different position will probably be confined to a relatively small region. Hence, this problem lends itself to the application of modern control theory and, in particular, linear quadratic regulator (LQR) theory.

A rather general linear optimal control problem may be stated as follows: Given the dynamic constraint equations

$$\dot{x} = Ax + Bu \tag{15}$$

find the control $u$ that satisfies Eq. (15) and minimizes the performance index

$$J = \tfrac{1}{2}(x_f - z_f)^T S_f (x_f - z_f) + \frac{1}{2}\int_{t_0}^{t_f} \left[(x - z_r)^T Q (x - z_r) + u^T R u\right] dt \tag{16}$$

where $S_f$ and $Q$ are positive-definite or semidefinite matrices and $R$ is a positive-definite matrix. Here, $z_r$ is a reference trajectory of the state during the maneuver and $z_f$ is a desired state at the final time $t_f$.

There may be additional constraints on the state and control. Because the tether cannot resist compression (tether slack), we may have constraints of the form

$$\epsilon_j \geq 0, \qquad j = 1, 2, \ldots, n$$

Also, the deflection of the aerodynamic control surfaces and/or the magnitude of the thrusting forces may be limited. Then,

$$u_{\min} \leq u \leq u_{\max}$$

We do not consider these types of constraints in this paper, because we think the problem of tether slack is more likely to happen during deployment or retrieval than during station keeping or maneuvers.

### Station Keeping

For the station-keeping control, we choose a typical LQR performance index

$$J = \frac{1}{2}\int_0^\infty (x^T Q x + u^T R u)\, dt \tag{17}$$

Then, the control $u$ is given by

$$u = -R^{-1}B^T S x = -Kx \tag{18}$$

where the matrix $S$ is the solution to the nonlinear algebraic matrix equation[10,11]

$$-SA - A^T S + SBR^{-1}B^T S - Q = 0 \tag{19}$$

After obtaining the optimal gain matrix $K$ we can use the control $u$ in conjunction with the nonlinear equations of motion [Eq. (9)]. In the simulation, the effect of the rotation of the atmosphere was added to produce unmodeled perturbing forces. In addition, the orbit of the main satellite is nonequatorial with inclination, $i = 23.5$ deg. This is one way of testing the effectiveness and robustness of the controllers because the linear analysis is based on an equatorial, circular orbit.

Shown in Figs. 6–11 are time histories of state variables of the system to initial-rate perturbations. Both controllers are quite capable of stabilizing the otherwise unstable motion. With a reasonable magnitude of control surface deflection or reaction thrust and torque, the in-plane and out-of-plane motions are effectively damped out

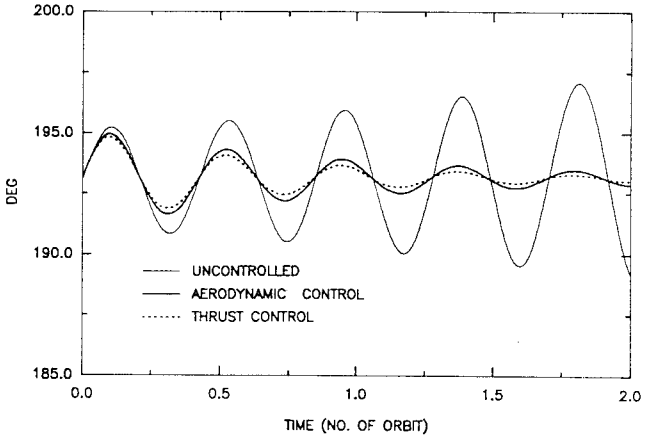


**Fig. 6 Time history of in-plane motion during station keeping.**

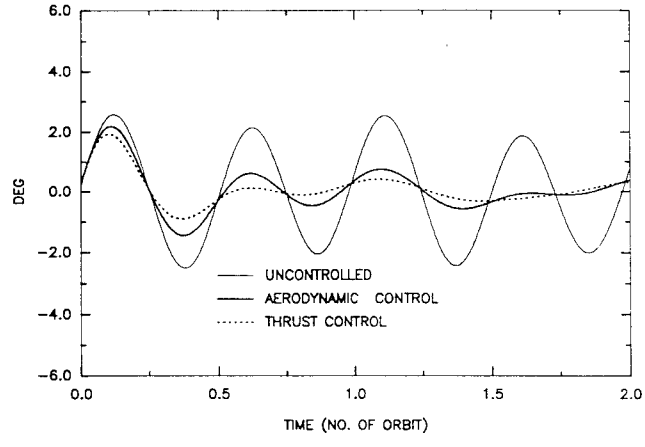


**Fig. 7 Time history of out-of-plane motion during station keeping.**

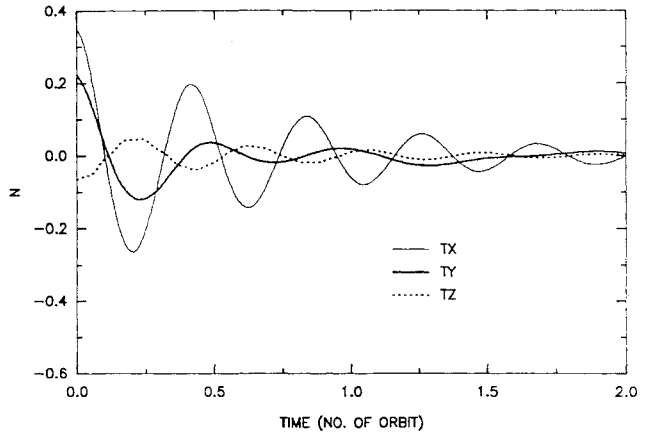


a) Aerodynamic control

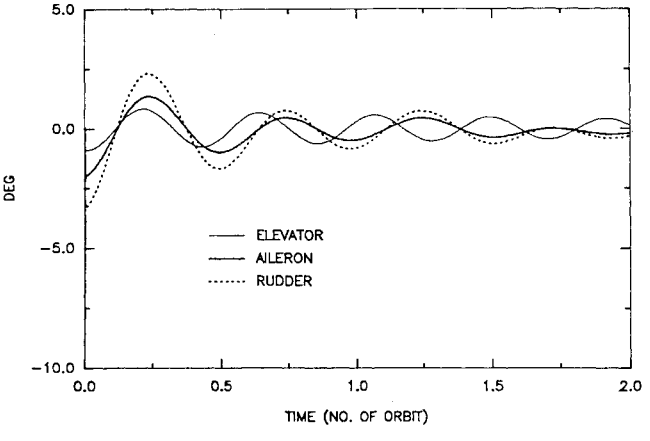


b) Thrust control

**Fig. 8 Time history of control activity during station keeping.**

within two orbits (see Figs. 6–8). However, the pitch and yaw responses in the controlled motion are much larger than those in the uncontrolled motion, as shown in Figs. 9 and 10. This is because relatively larger control deflections are required for the control of the translational motion than are needed for the control of attitude motions. The motion along the tether longitudinal direction is also well controlled (see Fig. 11).

In conclusion, the results clearly show that aerodynamic control may be used in station keeping and is as effective as reaction-type control, provided, of course, that the subsatellite is low enough in the atmosphere.

### Maneuvers

During a maneuver, if we are interested primarily in the final position of the tethered vehicle, we may use a performance index of the form

$$J = \tfrac{1}{2}(\boldsymbol{x}_f - \boldsymbol{z}_f)\boldsymbol{S}_f(\boldsymbol{x}_f - \boldsymbol{z}_f) + \frac{1}{2}\int_{t_0}^{t_f} [\boldsymbol{x}^T\boldsymbol{Q}\boldsymbol{x} + \boldsymbol{u}^T\boldsymbol{R}\boldsymbol{u}]\,\mathrm{d}t \quad (20)$$

There are several methods available to solve the problem of interest.[10,11] Using the usual procedure of forming the variational Hamiltonian and taking the required partial derivatives, we obtain the necessary conditions:

$$\dot{\boldsymbol{x}} = \boldsymbol{A}\boldsymbol{x} - \boldsymbol{B}\boldsymbol{R}^{-1}\boldsymbol{B}^T\boldsymbol{\lambda}, \quad (21a)$$

$$\dot{\boldsymbol{\lambda}} = -\boldsymbol{A}^T\boldsymbol{\lambda} - \boldsymbol{Q}\boldsymbol{x} \quad (21b)$$

with the initial conditions $\boldsymbol{x} = \boldsymbol{x}(t_0)$, $\boldsymbol{\lambda}_0 = \boldsymbol{S}(t_0)\boldsymbol{x}(t_0) + \boldsymbol{s}(t_0)$. For

$$\dot{\boldsymbol{S}} = -\boldsymbol{S}\boldsymbol{A} - \boldsymbol{A}^T\boldsymbol{S} + \boldsymbol{S}\boldsymbol{B}\boldsymbol{R}^{-1}\boldsymbol{B}^T\boldsymbol{S} - \boldsymbol{Q}, \qquad \boldsymbol{S}(t_f) = \boldsymbol{S}_f \quad (22)$$

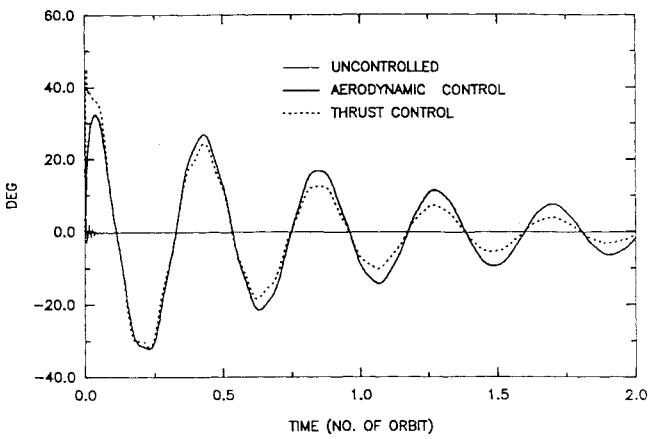


**Fig. 9 Time history of pitching motion during station keeping.**

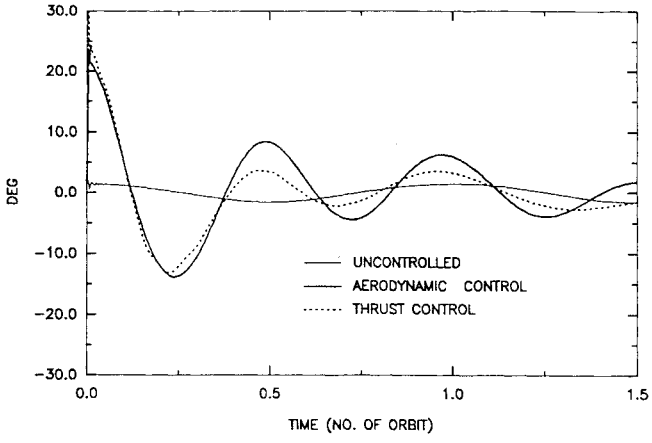


**Fig. 10 Time history of yawing motion during station keeping.**

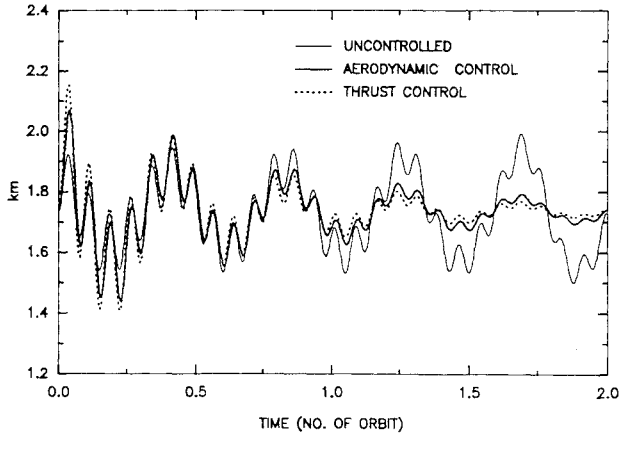


**Fig. 11 Time history of tether longitudinal motion during station keeping.**

a given final state $\boldsymbol{z}_f$ and weighting matrix $\boldsymbol{S}_f$, the matrix $\boldsymbol{S}(t_0)$ and vector $\boldsymbol{s}(t_0)$ are obtained when we integrate the following matrix and vector differential equations backward from $t_f$ to $t_0$:

$$\dot{\boldsymbol{s}} = -\boldsymbol{A}^T\boldsymbol{s} + \boldsymbol{S}\boldsymbol{B}\boldsymbol{R}^{-1}\boldsymbol{B}^T\boldsymbol{s}, \qquad \boldsymbol{s}(t_f) = \boldsymbol{S}_f\boldsymbol{z}_f \quad (23)$$

For the maneuver example, we considered two maneuvers of different magnitudes and durations. In the first, the in-plane and out-of-plane angles were each changed by 1 deg in 2000 s. The other states were to be kept at their equilibrium values which correspond to the initial position, $x = -24.55$, $y = 0$, $z = -98.73$ km, in the local vertical coordinate system. As in the station keeping case, the orbit of the main body was assumed to be equatorial and circular. In the second maneuver, the magnitude of the change in each of the in-plane and out-of-plane angles was 2 deg and the maneuver was accomplished in 3000 s.

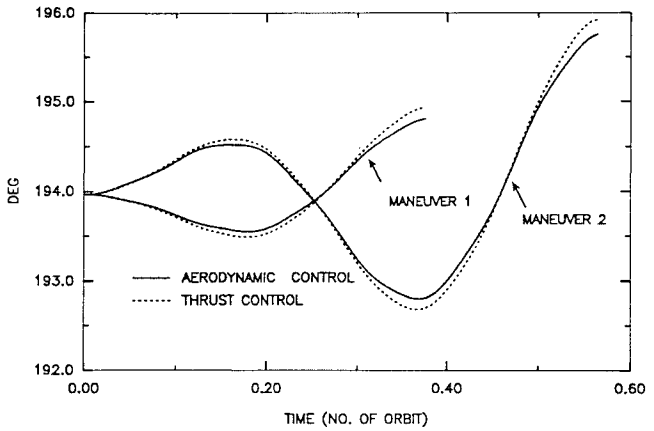


Fig. 12 Time history of in-plane motion during maneuver.

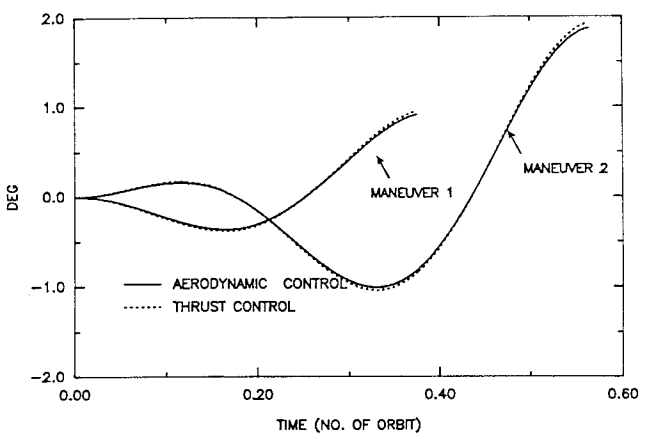


Fig. 13 Time history of out-of-plane motion during maneuver.

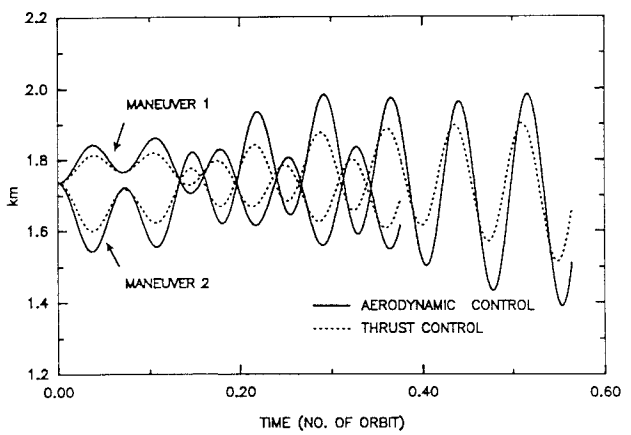


Fig. 14 Time history of tether longitudinal motion during maneuver.

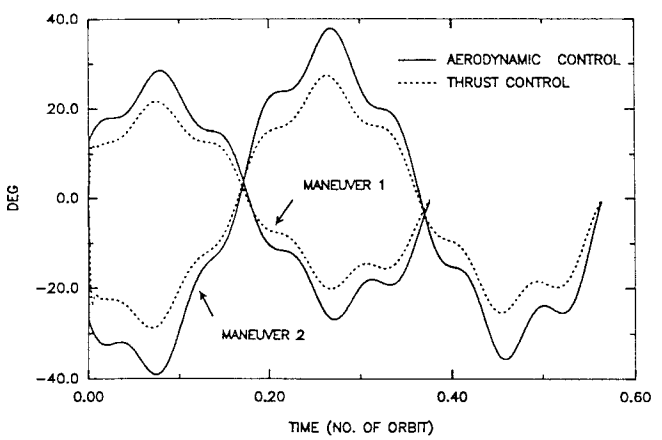


Fig. 15 Time history of pitching motion during maneuver.

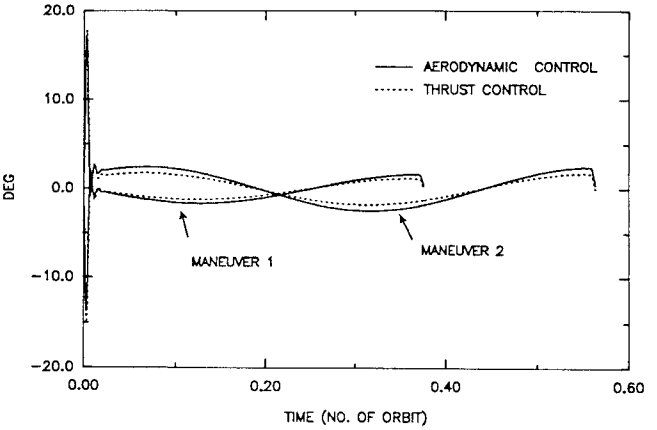


Fig. 16 Time history of yawing motion during maneuver.

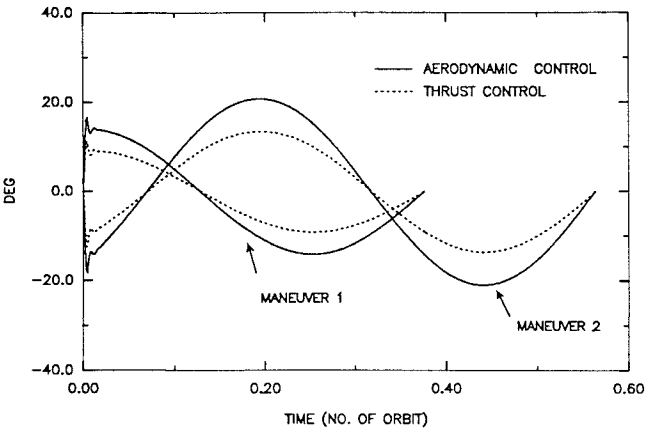


Fig. 17 Time history of rolling motion during maneuver.

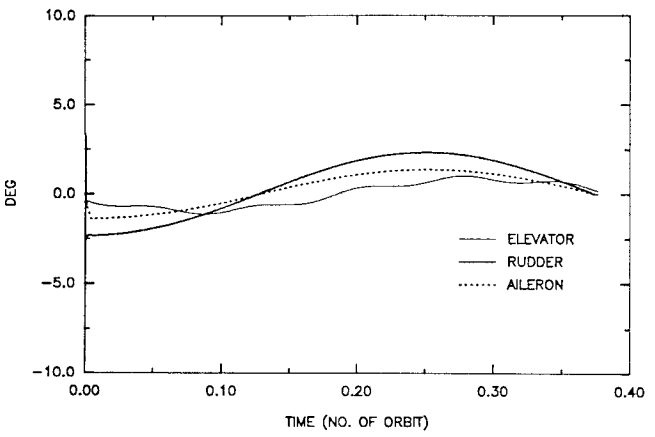


a) Aerodynamic control

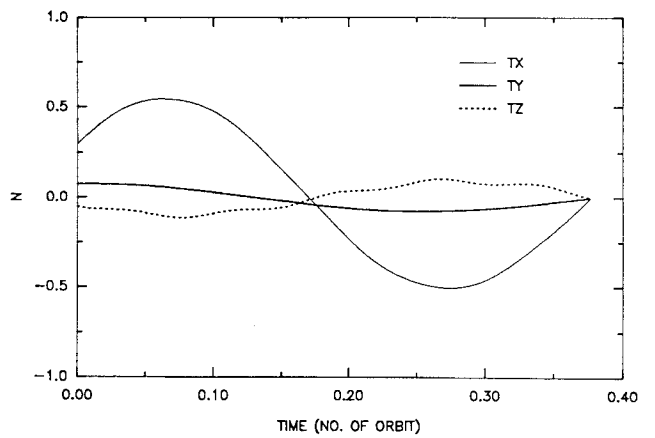


b) Thrust control

Fig. 18 Time history of control activity during maneuver 1.

Aerodynamic and reaction control results are shown here for comparison. Referring to Figs. 12–14, we see that the tethered vehicle has been successfully maneuvered close to the new position in each case. Interestingly, the vehicle was pushed forward (in the direction of flight) initially, then moved rearward in this example (Fig. 12). The attitude motion of the vehicle was somewhat active during the maneuver but finally settled down, as shown in Figs. 15–17. As shown in Fig. 18, the magnitudes of the control surface deflections and the reaction thrust and torque, respectively, remained reasonable during the maneuvers.

## Conclusions

Certain problems of dynamics and control of tethered flight vehicles were dealt with in this paper. The rather complicated equations of motion have been numerically linearized to produce state and control matrices that can be used quite effectively in the dynamics analysis and control synthesis. In the presence of atmospheric perturbations, the motion of a tethered system was shown to be unstable in certain cases. We considered the use of conventional control surfaces, such as elevator and rudder, as a means for subsatellite control. Modern control theory was employed to obtain appropriate control strategies for station keeping and maneuvering of the vehicle. Comparisons of the two different types of controller were made. To validate the numerical linearization and test the control schemes developed, the nonlinear equations of motion were integrated and the time histories of some significant variables were presented. The results indicate that, under appropriate circumstances, aerodynamic control is a viable alternative to reaction control for station keeping and maneuvering.

## References

[1]Misra, A. K., and Modi, V. J., "A Survey on the Dynamics and Control of Tethered Satellite Systems," *Advances in Astronautical Sciences*, Vol. 62, 1987, pp. 667–719.

[2]Banerjee, A. K., and Kane, T. R., "Tethered Satellite Retrieval with Thruster Augmented Control," *Journal of Guidance, Control, and Dynamics*, Vol. 7, No. 1, 1984, pp. 45–50.

[3]Pines, D. J., von Flotow, A. H., and Redding, D. C., "Two Nonlinear Control Approaches for Retrieval of a Thrusting Tethered Subsatellite," *Journal of Guidance, Control, and Dynamics*, Vol. 13, No. 4, 1990, pp. 651–657.

[4]Beletskii, V. V., and Levin, E. M., "Dynamics of the Orbital Cable System," *Acta Astronautica*, Vol. 12, No. 5, 1985, pp. 285–291.

[5]Onoda, J., and Watanabe, N., "Tethered Subsatellite Swinging from Atmospheric Gradient," *Journal of Guidance, Control, and Dynamics*, Vol. 11, No. 5, 1988, pp. 477–479.

[6]Bainum, P. M., and Kumar, V. K., "Optimal Control of the Shuttle-Tethered-Subsatellite System," *Acta Astronautica*, Vol. 7, 1980, pp. 1333–1348.

[7]de Matteis, G., and de Socio, L. M., "Stabilization of a Tethered Subsatellite System by Thrusters in Station-Keeping," American Astronautical Society Paper 91-173, Feb. 1991.

[8]No, T. S., and Cochran, J. E., Jr., "Dynamics and Stability Analysis of an Orbiter-Tether-Maneuverable Subsatellite System," American Astronautical Society Paper 91-172, Feb. 1991.

[9]Drummond, A. M., "Performance and Stability of Hypervelocity Aircraft Flying on a Minor Circle," UTIAS Report 135, Dec. 1968, Univ. of Toronto, Toronto, ON, Canada.

[10]Kirk, D. E., *Optimal Control Theory—An Introduction*, Prentice-Hall Englewood Cliffs, NJ, 1970, Chap. 5.

[11]Theodore, F. E., *Estimation and Control of Systems*, Van Nostrand Reinhold, New York, 1984, Chap. 6.